Interaction of hydrogen with the Be(0001) surface

Roland Stumpf and Peter J. Feibelman
Sandia National Laboratories, Albuquerque, New Mexico 87185-0344
(Received 20 December 1994)

Extensive first-principles calculations of the H-Be interaction reveal that novel H-surface vacancy structures dominate the high-coverage regime, from 2/3 to 1 monolayer (ML). At 1 ML the low-energy structure is a honeycomb of Be vacancies each decorated by three bridge-bonded H's tilting inward. At 2/3 ML the H's tilt in toward linear trenches organized in a 3×1 structure. At low coverages H prefers ordinary hcp threefold sites. A combination of the three structural models explains most of the experimental results. The adsorption of H in subsurface sites is shown to be unlikely.

I. INTRODUCTION

The H-Be(0001) adsorption system involves the simplest of adatoms interacting with an *sp*-bonded, or "simple" metal. Nevertheless, attempts to apply modern surface experimental probes to the structure of this technologically significant adsorption system have so far produced more confusion than enlightenment.[1–6] Because of the generally close relation between materials' structure and behavior, progress in surface science depends on reliable surface crystallography. Thus, it is important to respond to challenges, e.g., those presented by H/Be(0001) to the idea that modern experimental methods make the determination of surface atomic arrangements routine.

The most striking difficulty regarding H/Be(0001) concerns the work function change $\Delta\Phi$. Feibelman's first-principles electronic-structure calculations[6] imply work function changes in the neighborhood of -2 eV for 1×1 overlayers of H/Be(0001) in any of several adsorption geometries. The stark contradiction between this result and the value of $\Delta\Phi = -0.4$ eV measured by Ray, Hannon, and Plummer at saturation coverage (about 1 ML) is a strong indication that the 1×1 geometries assumed in the calculations are far from the actual H/Be bonding configuration.

In the work reported here, we resolve the work function puzzle as well as a variety of other experimental and theoretical paradoxes. We systematically investigate a large number of possible H bonding configurations. For the high-coverage limit, we show that H-induced vacancy reconstructions in which H adatoms sit on bridge sites tilted toward surface vacancies have the lowest total energy. The predicted structures represent a form of H-induced surface reconstruction.

The vacancy structures are only favorable at high H coverages (from 2/3 to 1 ML). At low coverage the adsorption geometry is more conventional – threefold hexagonal-close-packed (hcp) sites are occupied with little change in the underlying lattice. Because of the low diffusion barriers between the hcp sites, we expect disorder in the H adlayer except at the lowest temperatures.

Our calculations of H in several subsurface structures make it appear unlikely that subsurface H has been observed in the above-mentioned experiments. We find, however, a structure involving two monolayers of H, which might be metastable and a precursor for H-induced ablation.

Outline

We first give (Sec. II) a summary of what we currently know of the H on Be(0001) system. In Sec. III we describe our first-principles calculations. We continue (Sec. IV) with results for H on Be(0001) at different coverages on flat Be(0001). The coverage dependence of the adsorption energy and of the work function is discussed. As an alternative to on-surface H adsorption, we treat subsurface adsorption geometries. Then, in Sec. V we present our results for the H-induced 1×3 and $\sqrt{3}\times\sqrt{3}R30°$ vacancy structures. The H-$\sqrt{3}\times\sqrt{3}R30°$ structure turns out to be the most stable at high coverages. In Sec. VI we summarize, by sketching a phase diagram for H on Be(0001). Appendix A is a review of our calculations of the clean Be(0001) surface. There, we discuss the importance of numerical convergence and the differences of bonding in the bulk and at the surface, and we derive a model for the expansion of clean Be(0001). In Appendix B we discuss the fact that H adsorbed on flat Be(0001) does not remove the surface expansion.

II. HISTORY

Besides the work function puzzle (the work function reduction is much smaller in experiment than in theory), there are several other contradictions between H-Be(0001) experiments[1–4] and theory[5,6] and among different experiments. Most of this was discussed at length in Ref. 6, so we will only briefly discuss the situation here.

A. Results that make no sense yet

(1) The calculations of 1 ML H predict a 2.3 eV work function reduction.[6] In experiment the reduction is only 0.4 eV.[1] Thus, experiment and theory investigated a dif-

ferent structure. The change of Φ indicates a partially ionic character of the H-Be bond, i.e., charge is transferred from H to Be. This should lead to an electrostatic repulsion between neighboring H adsorbates and prevent the formation of 1×1 H islands.

(2) Theory predicts that the bridge site is favorable. High resolution electron-electron loss spectroscopy (HREELS) by Ray, Hannon, and Plummer (RHP) indicates that a *tilted* bridge site should be occupied at high coverages.[1]

(3) For 1 ML H on bridge sites, the clean Be(0001) surface state, which lies above the surface projected bulk bands, is removed in the whole surface Brillouin zone (SBZ).[6] Instead a surface band below the projected bulk band appears. This theoretical result disagrees with the angular-resolved ultraviolet photoemission spectroscopy (ARUPS) performed by Ray, Pan, and Plummer.[2] At a presumed coverage of 0.4 ML of H on Be(0001) the surface state of the clean surface is not completely removed. In most of the SBZ it just shifts to lower energies, while still staying above the bulk bands. A surface state below the bulk band appears in the remaining parts of the SBZ. This H-induced state is connected by a surface resonance in between.

(4) The photoemission data are in themselves hard to understand, because they show a 1×1 dispersion of the H associated surface states. At a coverage of 0.4 ML, this would mean that 40% of the surface is in a condensed 1×1 phase and that 60% of the surface is clean. 1×1 H islands should be unfavorable because of the electrostatic H-H repulsion. Furthermore, the clean fraction of the surface should give rise to the observation of the surface state of the clean surface, but it does not.

(5) The Be(0001) phonon dispersion observed in the presence of an H overlayer (coverage 0.4 ML) also contradicts the formation of 1×1 H islands.[1] Ray, Hannon, and Plummer observe that the clean surface phonon at the $\bar{M}$ point is folded back to the Γ point upon H adsorption. Thus, the surface unit cell is larger than 1×1.

In sum, the present understanding of the H-covered Be(0001) surface is far from satisfactory. In this paper, we resolve problems 1 and 2 in detail and we offer some ideas on how to resolve points 3–5.

B. Suggested ideas

Feibelman proposed in Ref. 6 that the 1×1 dispersion in both low-energy electron diffraction (LEED) and ARUPS, as observed experimentally,[1,2] is created by a disordered overlayer of H adsorbates at lower coverage. This disordered H overlayer should only increase the diffuse LEED background and not change the symmetry. The Be surface states should only be perturbed by a smeared-out H potential, whose strength is determined by the H coverage.

But several other pieces of experimental information suggest that the H/Be(0001) bonding configuration is actually far from the usual overlayer structures. One clue comes from the HREELS study of RHP.[1] The high H vibrational frequency observed there is indicative of a low coordination adsorption site, with rather strong bonds. This requirement is most likely fulfilled in a steplike geometry, as shown for the adsorption of H on a stepped Al surface.[7] If the density of steps were high enough, we could have the additional phase right there. However, well-prepared close-packed metal surfaces generally have too small a density of steps to explain the strong signal for the high frequency H vibrations seen in HREELS.

A steplike geometry is also realized at a surface vacancy. The formation of such a vacancy on a close-packed surface certainly costs energy. Recently, however, it was observed that adsorbates can sufficiently lower the energy for a vacancy structure so that it becomes stable on a close-packed surface.[8–10] In the first example, alkali-metal atoms sit quasisubstitutionally in the first layer of the Al(111) surface. Every third Al surface atom is removed so that the remaining atoms form a honeycomb mesh. It was found that such a $\sqrt{3}\times\sqrt{3}R30°$ arrangement of vacancies is especially stable.[9] The second example is the adsorption of Sb on Ag(111) in substitutional sites.[10] Is a similar vacancy structure realized on the Be(0001) surface and can it explain the observations made on H-covered Be(0001)?

C. New LEED data

The idea that vacancy structures may be important gains support from a recent LEED study by Pohl, Hannon, and Plummer (PHP).[4] Until recently it was reported that the LEED picture shows 1×1 symmetry, with some diffuse background for all coverages. In the latest experiments, the procedure has been changed. The H dosing is now performed at LN_2 temperature instead of room temperature, which perhaps allows for a higher H coverage. This leads to additional symmetries in the LEED patterns. When the crystal is heated after the dosing, a weak $\sqrt{3}\times\sqrt{3}R30°$ LEED superstructure starts to appear at $-20°$ C and is most intense at 0° C. Starting at around 50° C PHP observe a weak 1×3 LEED pattern. Thermal desorption spectroscopy shows that upon transformation from the $\sqrt{3}\times\sqrt{3}R30°$ to the 1×3 structure roughly 1/3 of the H atoms desorb. A LEED *I-V* analysis and an absolute coverage determination are the subject of another study.[4] We note that a $\sqrt{3}\times\sqrt{3}R30°$ LEED superstructure is also observed for "clean" (0001) oriented Be films grown on a Si(111) substrate.[11]

One should recognize that in exploring surface geometries, one generally keeps close to one's starting assumptions. For example, "relaxing" an overlayer geometry numerically, we will never arrive at a vacancy structure. But numerous clues from experiment suggest that H-Be structures are of that unusual kind. We have, therefore, systematically studied them and report the results in what follows.

III. ELECTRONIC-STRUCTURE CALCULATIONS

Our study is based on density-functional theory (DFT) with the local-density approximation (LDA) for exchange

and correlation (XC).[12] Electron wave functions are expanded in plane waves (PW) up to a cutoff of 20 Ry. The Be atoms are described by soft separable pseudopotentials (PP).[13,14] For the construction of the pseudopotential, we use cutoff radii of $r_s = r_p = r_d = 1.67$ bohr and a $2s^2 2p^0$ occupation of the atomic eigenstates. We use the d potential as the local potential, while treating the s and p potential nonlocally. We also use the partial core correction for XC with $r_c = 0.87$ bohr.[15] At this radius, the core charge density is three times the valence charge density. We test the quality of the pseudopotential and the basis set by using cutoff radii down to 1.1 bohr and plane wave cutoff energies up to 70 Ry. The H pseudopotential is constructed according to Refs. 16 and 17, treating the p potential as local. Its quality is demonstrated in Ref. 18.

Generally we use an orthorhombic supercell in our calculations. For comparison with the linear augmented plane wave calculations (LAPW) in Refs. 6 and 19 we have also used a hexagonal cell. We use special **k** points[20] and the Fermi surface smoothing technique of Methfessel and Paxton with a width of 0.2 eV to do the Brillouin zone (BZ) integration.[21] For different supercell sizes, we generate equivalent **k**-point meshes by folding of **k** points according to the supercell size.

Our standard **k**-point mesh is equivalent to a mesh of 72 special **k** points in the irreducible 1/8 of the BZ of a four atom bulk primitive cell. In the surface calculations we normally use the equivalent of 18 **k** points in the irreducible 1/4 of the SBZ of a two atom surface cell. We test convergence using up to four times the standard number of **k** points.

We integrate the Kohn-Sham equations via iterative minimization using steepest descent.[22–24] For the calculations of the Be(0001) surface we use a repeated slab of at least nine layers thickness, separated typically by five layers of vacuum. The outer three Be layers and the H adlayers on both sides are relaxed using a damped Newton dynamics technique.[24] The two surfaces of the slab are equivalent; we enforce mirror symmetry relative to the center plane of the slab.

IV. H ADLAYERS ON FLAT Be(0001)

We start our investigation of H adsorption on flat Be(0001) with the simplest case, 1 ML H coverage. Our results are essentially like the two earlier calculations (see Appendix B). We find (see Table I) that the bridge site is the most favorable with an adsorption energy $E_{ad} = 1.70$ eV. The fcc site is second ($E_{ad} = 1.61$ eV) and the hcp site is third ($E_{ad} = 1.56$ eV).[25] The H-Be bonds for H on the bridge site are obviously much stronger and they are shorter (2.8 bohr as compared to 3.0 bohr for the fcc site) than at the threefold sites.

We observe a reduction of the work function by 2.3 eV for 1 ML of H adatoms on the bridge site. This work function change is due to a polarization of electronic charge away from the H adlayer towards the Be surface. The net positive charge of the H atoms leads to an electrostatic H-H repulsion.

A. Coverage dependence of the adsorption energy of H on flat Be(0001)

The adsorbate-adsorbate interaction is in fact repulsive. The adsorption energy decreases with coverage from 2.52 eV for 1/12 ML to 2.24 eV for 1/3 ML to 1.70 eV for 1 ML of H (see Table I and Fig. 1).

This strong adsorbate-adsorbate repulsion poses questions of what the saturation coverage will be, and if 1 ML coverage as assumed by RHP (Ref. 1) can really be achieved for the H on flat Be(0001). Thermodynamically the saturation coverage is reached when the differential adsorption energy $\tilde{E}_{ad}$

$$\tilde{E}_{ad}(\Theta) = E_{ad}(\Theta) + \Theta \frac{\partial E_{ad}(\Theta)}{\partial \Theta} \tag{1}$$

is smaller than half the H_2 binding energy.[26] $\tilde{E}_{ad}(\Theta)$ is the energy gain when one isolated H atom is added to a H adlayer of coverage Θ. The derivative in Eq. (1) can be approximated by linear interpolation of ad-

TABLE I. Properties of H adlayers on flat Be(0001) at different coverage and at different adsorption sites. We list the adsorption energy per H atom E_{ad} in eV (defined relative to 1 Ry for the free H atom), the nearest-neighbor H-Be distance d_{H-Be} in bohr, the height h_H of the H adsorbate above the substrate nearest neighbors in bohr, the average relaxation of the two top layers Δd_{12} and Δd_{23} in percent of the ideal interlayer spacing of 3.326 bohr, the work function Φ in eV, and the adsorbate-induced surface dipole μ in debye.

Coverage (ML)	H unit cell	Site	E_{ad} (eV)	d_{H-Be} (bohr)	h_H (bohr)	Δd_{12} (%)	Δd_{23} (%)	Φ (eV)	μ (debye)
1	1×1	fcc	1.61	3.00	1.74	3.0	0.4	3.60	0.22
		bridge	1.70	2.81	1.84	2.6	0.3	3.20	0.26
		hcp (Ref. 25)	1.56	3.02	1.78	2.3	0.6	3.10	0.28
1/3	$\sqrt{3} \times \sqrt{3}R30°$	fcc	2.19	2.99	1.72			4.59	0.32
		bridge	2.05	2.81	1.85			4.60	0.31
		hcp	2.24	2.96	1.67	2.3	1.0	4.56	0.33
1/12	$2\sqrt{3} \times 3$	bridge	2.35	2.79	1.80			5.29	0.32
		hcp	2.52	2.95	1.57	2.5	1.0	5.27	0.35

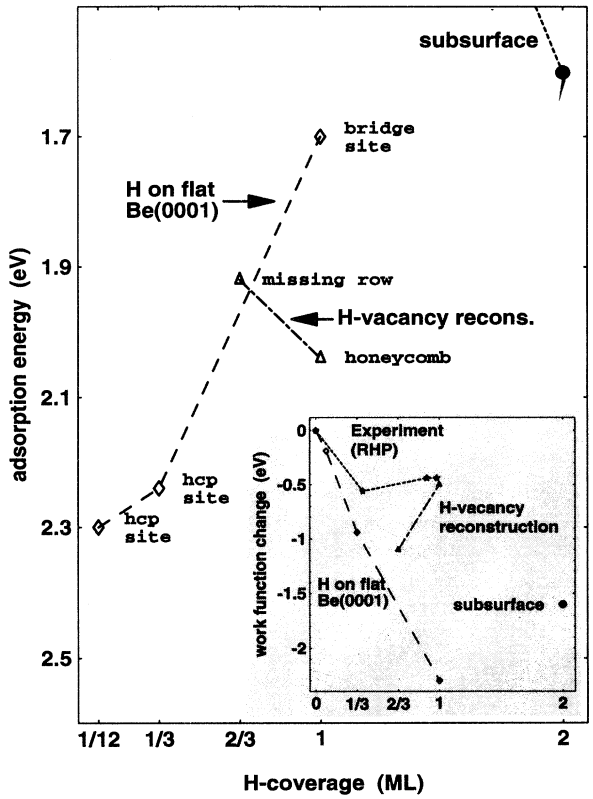

FIG. 1. H adsorption energy as a function of coverage for the three different H on Be(0001) phases discussed in the text; the inset shows the corresponding work function changes and compares it with the experimental values of RHP (Ref. 1).

sorption energies at the calculated coverages. We get $\tilde{E}_{\rm ad}(1/12\ {\rm ML}) \approx 2.3$ eV, $\tilde{E}_{\rm ad}(1/3\ {\rm ML}) \approx 1.9$ eV, and $\tilde{E}_{\rm ad}(1\ {\rm ML}) \approx 1.2$ eV.

These values should be compared to 2.38 eV, i.e., half the experimental H_2 binding energy.[27] This comparison leaves no doubt that thermodynamically the high-coverage phases are unstable against desorption. This analysis, however, does not include the barrier for the recombination and desorption of H. It might cause high-coverage H adlayers to be metastable.

B. Coverage dependence of the work function

To reduce the electrostatic energy, the H-Be bond partially depolarizes at high coverages. The dipole moment per H adatom is smallest at the highest coverage (0.26 debye at 1 ML compared to 0.35 debye at 1/12 ML). The depolarization, however, is not strong enough to lead to work function saturation. This disagrees with the experimental observations of RHP (Ref. 1) as can be seen in the inset of Fig. 1.

The fact that the work function does not saturate is in marked contrast to the otherwise similar case of the alkali adsorption. Alkalis also have one valence electron, and reduce the work function on most surfaces. However they show work function saturation. The saturation is accompanied by the formation of bonds within the adsorbate layer.[9,28] H cannot establish in-plane bonds to its H neighbors and chemically bind to the surface at the same time. This would require that the H-H bonds adopt some p character. This is too costly because of the extremely high s to p promotion energy of 3/4 Ry.[29]

C. Adsorption sites

On the flat Be(0001) surface, the equilibrium adsorption site is coverage dependent. At 1 ML, it is the bridge. At 1/3 ML and lower coverage, it is the hcp site. Other sites like the top or tilted bridge sites are not local minima, whereas the fcc sites always are local minima.

The fact that the bridge site can be an equilibrium site on a close-packed metal surface first comes as a surprise. According to Ref. 6 the reason is that on the bridge, the H atoms interact especially strongly with the dangling bond like p_σ orbitals of the Be surface atoms. Those orbitals point out of the surface. At lower coverage the low-energy site switches to a threefold coordinated site because this leaves less Be surface atoms without H neighbors. The reason why the hcp site has a lower energy than the fcc site is not known in this or any other case.[7,30]

D. The dilute phase of H on Be(0001)

As mentioned before, it is likely that the H saturation coverage for the on-surface phase is well below one monolayer. We must therefore consider the properties of a submonolayer H adsorbate phase.

Down to fairly low temperatures, H adsorbed on the flat Be(0001) surface will show a fluidlike behavior. This is a consequence of the low diffusion barrier, which we find for H adatoms on Be(0001) at 1/3 ML and 1/12 ML (see Table I). Assuming that the bridges sites are the saddle points for surface diffusion, and neglecting adsorbate-adsorbate interaction and effects of zero-point vibration, the calculated diffusion barriers are 0.17 eV for 1/3 ML and 0.14 eV for 1/12 ML H. Close to 300 K, where most of the experiments were done, these barriers might be too small to stabilize order within the H adlayer.[31]

Certainly the neglect of adsorbate-adsorbate interaction is questionable for H on Be(0001). Especially in the 1/3 ML coverage case, the H-H repulsion will increase the apparent diffusion barriers. A detailed study of the effect of the H-H repulsion, however, will have to take into account complicated processes of concerted motion of a number of H adatoms with low diffusion barrier. This remains to be done. The same is true for quantum effects in the motion of the H adsorbates.

In a dilute H adlayer on flat Be(0001) LEED, HREELS, and ARUPS experiments must all yield 1×1 dispersion. This would explain some of the experimental observations. In LEED only the diffuse background should be increased by the dilute H adlayer.

The H-induced surface phonon features, as measured for example with HREELS, should be very broad because

of the weak localization of the H adatoms. We expect the strongest signal in HREELS from the perpendicular vibration of a H adatom on the hcp site. We determine the energy for that vibration at 1/3 ML coverage to be 150 meV. The rather sharp features observed in HREELS by RHP at energies higher than 150 meV (Ref. 1) most likely originate, therefore, from the H-induced vacancy structures that we discuss later.

Angular-resolved ultraviolet photoemission spectroscopy experiments done on the dilute H phase should reveal the clean Be(0001) surface states, however, shifted to lower energies, because of the additional attractive potential coming from the H adlayer. This potential can be approximated within the virtual crystal model.[32]

E. Subsurface H

Whether or not Be absorbs H is an important issue for the use of Be as inner wall material of Tokamak fusion reactors.[3] H absorption might lead to Be embrittlement, for example, and also to Be ablation into the plasma. We do not know, however, if H does go into subsurface layers. Subsurface adsorption was recently proposed as a factor to explain thermal desorption spectroscopy measurements[3] and to explain the discrepancies between measured and calculated properties of H adlayers on Be(0001).[6] On the other hand, because of the high valence charge density in Be, the highest among the *sp* metals, any stable subsurface site for H is very unlikely.[33]

The energetics of 1 ML of H adatoms moving to an octahedral subsurface site has been investigated in a LDA calculation by Yu and Lam.[5] They find that the subsurface site is unfavorable by 1.4 eV and that the barrier to get there is 1.6 eV. The atoms were not allowed to relax in that calculation. We investigate layers of subsurface H (1 ML, 1/2 ML, and 1/4 ML) at an otherwise clean surface and at a surface precovered by 1 ML of on-surface hydrogen. We allow the atoms of the top three layers to relax and look both at tetrahedral and octahedral subsurface sites. Our findings confirm Yu and Lam's results. With one exception, H is about 1 eV less well bound in subsurface sites as compared to on-surface sites.

The exception is a structure, where 2 ML of H are adsorbed. 1 ML of H atoms resides at fcc sites on Be(0001). A second H monolayer, the subsurface H, is located between the outermost and the second Be layer at tetrahedral sites, i.e., on top sites relative to the second Be layer. The separation between the top two Be layers is increased by 70% relative to the clean surface. Because of this large separation one can speculate that this H-Be-H sandwich structure is a precursor in the process of H-induced ablation of Be(0001).

The H adsorption energy for the H-Be-H sandwich is 1.6 eV. This is close to the adsorption energy of 1 ML H on the flat surface (1.7 eV). The differential adsorption energy for the 2 ML structure is even about 1 eV larger, which means that it should be more stable against desorption.

We do not assume that the 2 ML subsurface structure has been realized experimentally. The work function for the H-Be-H sandwich structure is more than 1 eV lower than the measured work function of H-Be(0001).[1] Its energy is rather high compared to the low-energy H-induced vacancy structures we discuss in the next section.

V. H-INDUCED VACANCY STRUCTURES

Having thoroughly investigated the on-surface and subsurface H-Be(0001) structures, and having found that they do not resolve a host of experimental questions, we now discuss H-induced vacancy structures. Here, the reconstructed surface provides dangling bondlike orbitals which the H atoms passivate in a fashion reminiscent of H on semiconductor surfaces. In Table II we list those three H-induced vacancy structures which are lower or similar in energy, compared to H on the flat surface at the same coverage. We gain confidence that these three structures are the relevant high-coverage ones after having investigated more than twenty different structures involving Be vacancies and onefold, twofold, and subsurface H adatoms.

A. Honeycomb

The adsorption energy for H in the vacancy structures is highest (2.04 eV) for the $\sqrt{3}\times\sqrt{3}R30°$ honeycomb structure [see Fig. 2(a)]. One third of the Be(0001) surface atoms are removed in this structure. The remaining surface atoms build a $\sqrt{3}\times\sqrt{3}R30°$ honeycomb lattice. Every twofold site of this vacancy surface is occupied by a H adatom corresponding to 1 ML coverage.[34] The H adsorbates are all equivalent. They tilt towards the closest atom in the second Be layer, i.e., in the direction of the hcp site of the unreconstructed surface. Thus every vacancy is decorated symmetrically by three H atoms. The tilt angle is 40° relative to the surface normal and the H's height is reduced by 29% compared to the bridge adsorption on the flat surface at 1 ML.

One reason for the tilt of the H adsorbates is their electrostatic repulsion. By tilting away from the ideal bridge site, the H adsorbates increase their separation until they reach the next hcp or fcc site. The tilt stops shortly before the hcp site is reached.

The main driving force for the tilt, however, is covalent. If the H adatoms are put on the bridge site of the honeycomb surface with a tilt toward the fcc site and if they are then allowed to relax, these H atoms move spontaneously to the hcp side. This preference is clearly a covalent effect. The lowering of the H-H repulsion should be as effective in the fcc-tilted case as in the hcp-tilted case. It seems that the H atoms passivate Be orbitals that incline towards the hcp site.

B. Missing row

The 3×1 H-induced missing row reconstruction is formed by removing every third close-packed row of surface Be atoms, leaving Be double rows on the surface

TABLE II. Properties of three H-induced surface reconstructions on Be(0001). Every structure is characterized by its H coverage, the H adsorption sites (br.-hcp is for bridge tilted towards the hcp site of the ideal surface, br.-fcc is for bridge with tilt towards the fcc site of the ideal surface; *side* means beside row and on top site relative to second layer), the adsorption energy per H atom relative to the unreconstructed surface E_{ad} (i.e., with the removed Be surface atoms moved to bulk sites), and relative to the already reconstructed surface E_{bond} (i.e., the energy gain due to the H-Be bonds). The H reference energy is 1 Ry. We also give the shortest H-Be distance d_{H-Be}, the height h_H of the H adsorbates above the substrate nearest neighbors, the tilt angle θ of the H-Be bond relative to the surface normal, and the average relaxation of the top Be layers Δd_{12} and Δd_{23} in percent of the ideal interlayer spacing of 3.326 bohr. Φ is the work function [compare to 5.5 eV for the clean Be(0001) surface]. See also Fig. 1.

Coverage (ML)	Reconstruction	Sites	E_{ad} (eV)	E_{bond} (eV)	d_{H-Be} (bohr)	h_H (bohr)	θ (°)	Δd_{12} (%)	Δd_{23} (%)	Φ (eV)
1	$\sqrt{3}$ honeycomb	br.-hcp	2.04	2.72	2.72	1.31	40	4.5	1.1	5.0
2/3	3×1 miss. row	br.-hcp/br.-fcc	1.92	2.29	2.78/2.80	1.69/1.74	21/18	4.0	1.9	4.4
2/3	3×1 added row	br.-hcp/side	1.86	2.27	2.76/2.72	1.71/-0.54	14/—	−1.4	0.4	4.6

[see Fig. 2(b)]. The H coverage is 2/3 ML and the H adsorption energy is 1.92 eV. Again the H adsorbates sit on tilted bridge sites. They occupy all those bridge sites that border the vacancy rows, and they tilt towards the vacancies. One half of the H atoms tilts toward hcp sites of the flat surface [the ones which tilt to the left in Fig. 2(b)], the other half tilts toward fcc sites. It appears that the H atoms tilting toward hcp sites are bound more strongly. They tilt farther and their H-Be bonds are shorter.

C. Added row

The third H-induced reconstruction of Be(0001) that we discuss here is of the added row type [see Fig. 2(c)]. The unit cell of the reconstruction is 3×1, the H coverage is 2/3 ML, and the adsorption energy is 1.86 eV. There are two inequivalent H adsorbates in this structure. One half cover the bridge sites of the Be row, tilting 14° towards the hcp site of the unreconstructed surface. This is rather similar to sites on the other two H-induced vacancy structures. The other half of the H adsorbates sit on top of a second layer Be atom and beside a Be atom of the added row. Their height is 0.54 bohr lower than that of the added row atoms. The on-top bond to the second layer Be atom is 1.5% shorter than the bond to the Be atom of the added row. The tilt angle of the H-Be bond relative to an ideal on the top position on the second layer Be is 10° in the direction away from the added row. The second layer Be atom bonded to the H relaxes outward relative to the other atoms of the second layer by 6%.

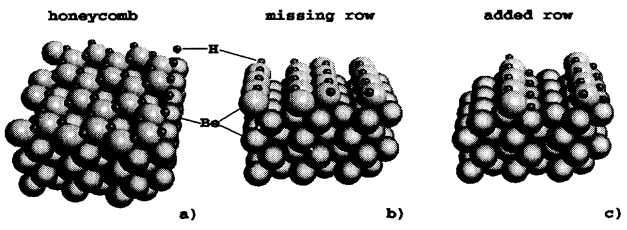

FIG. 2. Model of the three H-induced surface reconstructions discussed in the text.

D. Nature of the three vacancy structures without the H adlayer

The adsorption energy for the three H-induced vacancy structures can be broken into two contributions. One is the cost in energy to form the vacancy structure by removing the Be surface atoms and moving them to bulk equivalent sites like kinks (E_{form} in Table III). There the removed Be atoms gain the Be bulk cohesive energy. The other contribution is the energy gain in forming the H-Be bond on the reconstructed surface (E_{bond} in Table II). We will first discuss the formation of the vacancy structure.

The honeycomb vacancy structure on Be(0001), without the H adatoms, is energetically especially unfavorable. The vacancy formation energy in the honeycomb structure is 2.05 eV as compared to 0.73 eV for the missing row structure (see Table III).[35] The energy to create one 3×1 cell of the added row structure is also lower (0.82 eV).

There are two reasons for this difference. The first involves bond counting. To create one cell of the honeycomb structure from flat Be(0001) one removes a ninefold coordinated surface atom and puts it at a sixfold kink site, which means that three bonds are broken in this process. To build the missing row structure, only eight bonds have to be broken per removed atom (only in starting a row are nine bonds broken), which adds up

TABLE III. Comparison of flat and reconstructed Be(0001) with no H adsorbed. We quote the formation energy of the reconstruction E_{form} (with the removed atoms put to a bulk site) and the relaxation energy ΔE_{relax}, both per three atom surface cell. Δd_{12} and Δd_{23} are the average relaxation of the top two interlayer spacings in percent of the ideal interlayer spacing of 3.326 bohr. The slabs we use to model the reconstructed surfaces are nine layers thick, including the two defective layers.

Reconstruction	E_{form} (eV/cell)	ΔE_{relax} (eV/cell)	Δd_{12} (%)	Δd_{23} (%)
Flat Be(0001)		0.02	2.7	1.2
$\sqrt{3}$ honeycomb	2.05	0.02	-1.1	1.9
3×1 miss. row	0.73	0.30	-3.5	2.6
3×1 added row	0.82	0.14	-8.6	3.0

to two broken bonds per 3×1 cell. To create a cell of the added row structure, one removes a sixfold coordinated atom from a kink site and adds it at the fourfold site at the end of an added row. Again two bonds are broken relative to the flat Be(0001). A reasonable estimate of the energy gain by one Be-Be bond is 1/6 of the cohesive energy of hcp-Be, or 0.55 eV per bond.[36] Thus, about half of the difference in formation energy between the honeycomb and the two other structures comes from a different number of broken bonds. The other half has to do with surface stress and relaxation.

The flat Be(0001) surface is under tensile stress (0.2 eV/Å^2 = 2.6 eV per three atom cell, according to our preliminary calculations).[37] The stress tells us that the surface atoms want stronger in-plane bonds. In the honeycomb structure every second in-plane bond is broken and the remaining in-plane bonds are hindered from getting stronger because the symmetry does not allow them to get shorter. The energy gain by relaxation (E_{relax} in Table III) is therefore small. In fact it is as tiny as for flat Be(0001) (0.02 eV per three atom cell). The reduced symmetry of the missing and the added row vacancy structures, on the other hand, allows for a strengthening of in-plane bonds, explaining the rather large relaxation energy of 0.30 eV and 0.14 eV per 3×1 cell. It is instructive to compare the nature of the relaxation of the 3×1 reconstructions.

In the missing row structure, the paired rows reduce their separation by 12% of the ideal row-row distance. This reduces inter-row bond lengths by 9%. The strongly bonded paired rows relax inward by 3.5% and cause a rumpling of the second layer. Second layer atoms not covered by surface atoms relax outward by about 10% of the layer spacing relative to the covered atoms.

For the added row structure the relaxation can be described as the initial stage of incorporation of the added rows into the second layer. This reduces the bond length between the atoms of the added rows and their neighbors of the second layer and also the in-plane bond length within the second layer. The tensile surface stress should be effectively reduced for both 3×1 reconstructions after the relaxation.

It is interesting that for Al(111) the situation is very different. Al(111) is the only other *sp*-metal surface for which a similar analysis of the vacancy formation energy has been done.[9,30,38] At Al(111) the honeycomb structure is relatively stable. Its formation energy is only 0.36–0.41 eV (Refs. 9 and 38) as compared to 0.67 eV (Ref. 30) for the isolated vacancy and about 0.4–0.5 eV (Ref. 39) for the missing row structure. Vacancy formation on Al(111) costs two to five times less energy than on Be(0001) even though the cohesive energy of both elements is nearly identical.[40] Still, or perhaps as a result, these vacancy structures on Be(0001) can be stabilized by H passivation. Thus, the energetics of the alkaline-induced vacancy structures on Al(111) and of the H-induced vacancy structures on Be(0001) are quite different. In the alkaline-on-Al case a low vacancy formation energy favors the honeycomb structure, for H on Be(0001) it is the strength of the H-Be bond, as we will see.

E. Bonding of H to the vacancy structures

In general, more stable surfaces provide less stable adsorption sites. Thus H-Be bonds should be stronger in the $\sqrt{3}\times\sqrt{3}R30°$ honeycomb structure than in the 3×1 missing and added row structures, and this is what we find (see E_{bond} in Table II). In the H-$\sqrt{3}\times\sqrt{3}R30°$ structure the H-Be binding energy is about 0.44 eV bigger than for the two 3×1 structures. The stronger bonding is accompanied by a ca. 2% shorter H-Be bond length.

One reason for the weaker H-Be bond on the 3×1 reconstructions is that the relaxation of the clean vacancy structures is undone or even reversed (see Tables II and III) by the H adsorbates, which costs energy. The main reversal of the relaxation is that the nearest-neighbor distance in the double rows of the missing row reconstruction is changed from 9% below to 8% above the bulk nearest-neighbor distance.

We learned that the H adatoms are more strongly bound in the H-$\sqrt{3}\times\sqrt{3}R30°$ structure than in the H-3×1 structures. Additionally there are 3 H adatoms per surface cell in the H-$\sqrt{3}\times\sqrt{3}R30°$ structure which "pay" for the vacancy formation as compared to only 2 H adatoms in the 3×1 structures. We directly calculate that the number of H adatoms per cell is important. If only 2/3 ML of H is adsorbed on the $\sqrt{3}\times\sqrt{3}R30°$ structure, the adsorption energy per H atom is reduced from 2.05 eV to 1.82 eV, which makes the $\sqrt{3}\times\sqrt{3}R30°$ structure less stable than the H-3×1 structures. Those provide for adsorption energies of 1.92 eV and 1.86 eV.

The reduction of adsorption energy with reduced coverage means that the H-H interaction is net attractive in the H-$\sqrt{3}\times\sqrt{3}R30°$ structure as opposed to the H-H repulsion on the flat surface. Therefore, a condensation into the H-$\sqrt{3}\times\sqrt{3}R30°$ structure above a certain coverage can be expected. This H-$\sqrt{3}\times\sqrt{3}R30°$ structure will transform into the observed 3×1 structures when H atoms are removed, e.g., by evaporation.

A crude estimate of the differential adsorption energy $\tilde{E}_{\text{ad}}$ [see Eq. (1)] by using $E_{\text{ad}}(1\text{ ML}) = 2.04$ eV and $E_{\text{ad}}(2/3\text{ ML}) = 1.82$ eV gives a value of 2.6 eV for $\tilde{E}_{\text{ad}}$. This means that the H atoms in this structure should desorb at higher temperatures than the on-surface H atoms ($\tilde{E}_{\text{ad}} = 2.3$ eV at 1/12 ML). This agrees with the two thermal desorption peaks found by Lossev and Küppers.[3] They assign the high-temperature peak to subsurface H. We presume that it comes from the vacancy structures.

F. Work function

The work function reduction relative to the clean Be(0001) is much smaller for the H-induced vacancy structures than for H adlayers on the flat surface at the same coverage (see Fig. 1). The H-Be bonds are less ionic in the vacancy structures. The calculated work function of the H-$\sqrt{3}\times\sqrt{3}R30°$ phase is practically the same as that measured for H saturated Be(0001) by RHP.[1] This is a strong hint that the H-$\sqrt{3}\times\sqrt{3}R30°$ phase was the main phase present in experiment.

VI. PHASE DIAGRAM OF H ON Be

By combining our results for the different H phases considered above we can try to assemble a phase diagram for H on Be(0001).

A. Low temperature

At low temperature, so that no surface vacancies can form, the H adatoms will reside on the flat Be(0001) surface on hcp sites. The saturation coverage for the "H on flat Be(0001)" phase is very likely below one monolayer because of the strong H-H repulsion.

If there are preexisting steps on Be(0001) they will likely be decorated by H adatoms first, before the "H on flat Be(0001)" phase growth. Steps will provide the same kind of low-energy twofold binding sites as in the H-induced vacancy phases.

Above some temperature, the "H on flat Be(0001)" phase will be disordered. The low-energy barrier for H surface diffusion ($E_D \simeq 0.15$ eV) suggests that the order-disorder transition is at a "low" temperature. Disorder of the "H on flat Be(0001)" phase is also in agreement with the 1×1 dispersion, which is observed in ARUPS and LEED under certain conditions already at LN_2 temperatures.

B. High temperature

If the temperature is high enough that vacancies in the Be(0001) surface can be formed and that the removed Be atom can move to the next kink site, the H-$\sqrt{3}\times\sqrt{3}R30°$ phase will form. With increasing H coverage the H-$\sqrt{3}\times\sqrt{3}R30°$ phase will grow in size until the whole surface is covered. Below 1 ML coverage the H-$\sqrt{3}\times\sqrt{3}R30°$ and the disordered H on flat Be(0001) phase will coexist.

There is good reason to assume that the growth should start at preexisting steps. It is reasonable to assume that the barrier for vacancy formation in steps is lower than on the flat surface. At least this was found for Al(111).[30] Furthermore, Be atoms removed from the step do not have to diffuse far to find a low-energy adsorption site. The step itself provides them.

The barriers to creating the H-induced vacancy structures are reduced by the presence of the H adatoms. This H-assisted vacancy formation will be discussed in a forthcoming paper.[41]

We noted that the formation of the H-$\sqrt{3}\times\sqrt{3}R30°$ phase, is very likely an activated process and will therefore happen only above certain temperatures at observable rates. This temperature could, however, be above the temperature when H adatoms desorb at significant rates. This could prevent the formation of the H-$\sqrt{3}\times\sqrt{3}R30°$ phase. There are experimental indications that H desorption and the growth of the H-$\sqrt{3}\times\sqrt{3}R30°$ phase compete at the relevant temperature and coverage.[1,4] The observed H-induced $\sqrt{3}\times\sqrt{3}R30°$ LEED spots are weak and can only be seen after very careful control of dosage and temperature.[4] In order to produce a better ordered H-$\sqrt{3}\times\sqrt{3}R30°$ phase we propose that one deposit Be atoms during the H exposure. This way the vacancy structures should be able to grow at lower temperatures, which would reduce the H desorption rate.

Pohl, Hannon, and Plummer[4] showed that the H-$\sqrt{3}\times\sqrt{3}R30°$ phase transforms into a 3×1 phase upon heating to 370 K. This structural transformation is accompanied by a partial desorption of H, which reduces the coverage by about 1/3. This is in agreement with our calculations, at 2/3 ML coverage the H-3×1 structures are lower in energy than the H-$\sqrt{3}\times\sqrt{3}R30°$ structure.

VII. CONCLUSIONS

We have presented the results of our first-principles calculations of the unusual properties of H-covered Be(0001) surface. Our calculations identify several phases of H adsorbed on Be(0001): the H on flat Be(0001) phase, the H-$\sqrt{3}\times\sqrt{3}R30°$ honeycomb phase, and the H-3×1 missing and added row phases.

In the H on flat Be(0001) phase, the H coverage is well below 1 ML. The H adatoms sit in hcp sites, which are separated by only small diffusion barriers. This and some experimental observations (1×1 dispersion in LEED and ARUPS) indicate that this phase is disordered at least down to LN_2 temperatures. The H adatoms are positively charged relative to the substrate, which leads to a reduction of the work function and contributes to a strong H-H repulsion. The work function does not saturate with H coverage.

Our calculations rule out the idea that subsurface H contributes to the observed properties of H on Be(0001). However, we do find a Be-H-Be-H sandwich structure at the surface corresponding to 2 ML H coverage, which is metastable and might be important for H-induced ablation of Be.

At high H coverage, H-induced vacancy arrays, the first found on any surface, are the most stable structures. A H-$\sqrt{3}\times\sqrt{3}$ honeycomb geometry, where 1 ML of H atoms is adsorbed on tilted bridge sites, has the lowest energy of these H-vacancy arrays. The H-Be bonds are very strong and nearly covalent in the honeycomb geometry, which pays for the rather large energy of formation of the honeycomb array of vacancies. The H-H interaction in this structure is net attractive.

At a reduced coverage of 2/3 ML two H-induced 3×1 vacancy structures, one of the missing row, the other of the added row type, become energetically favorable. Again the H adatoms are twofold coordinated, the H-Be bonds are however slightly weaker. The energy of these geometries is low because the vacancy formation energy is small. Both the H-$\sqrt{3}\times\sqrt{3}$ honeycomb and the H-3×1 structures were observed in experiment.[4]

This work is an example of how modern first-principles calculations can solve the surface structure of a unique and complex adsorbate-surface system and how valuable insight into the physical driving forces of that adsorbate-surface system can be gained. There remain important

problems to be solved however. The H-induced surface phonons as measured in Ref. 1 should be calculated and discussed in more detail. The H-induced surface states with their 1×1 symmetry are not yet fully explained. It also would be desirable to know more about the important barriers for H desorption, for Be surface self-diffusion, and for vacancy formation on the flat surface and finally close to steps in the presence of H.

ACKNOWLEDGMENTS

We would like to thank Jim Hannon, Karsten Pohl, and Ward Plummer for the many discussions we had and for making available their results prior to publication. The work of R. Stumpf is supported by NEDO, The New Energy and Industrial Technology Development Organization of Japan. This work was also supported by the U.S. Department of Energy under Contract No. DE-AC04-94AL85000.

APPENDIX A: BULK Be AND CLEAN Be(0001)

Bonding in bulk-Be and at the Be(0001) surface is quite different.[42] Bulk hcp-Be is nearly a semiconductor, whereas the bonding at Be(0001) is much more metallic. Understanding this difference helps in understanding the adsorption of H on Be(0001). Investigating bulk Be and clean Be(0001) also permits tests of computational accuracy.

1. Results for bulk Be

We determine the hexagonal lattice constants a and c and the Poisson ratio ν_P in order to check the quality of our plane-wave basis set, the Be pseudopotential, and the **k**-point mesh for later use in the surface calculation. a, c, and ν_P are determined first by calculating the energy per atom for 16 pairs of values for the a-lattice constant and the c/a ratio. The resulting energy values are then used in a least squares fit of the ten coefficients of a general two-dimensional cubic polynomial. From this polynomial, we extract the equilibrium lattice constants a and c and the Poisson ratio ν_P. For the Be-pseudopotential, plane-wave cutoff, and **k**-space sampling as described in Sec. III, we get $a = 4.23$ bohr, $c/a = 1.573$, and $\nu_P = 0.025$.

Using a fully converged basis of plane waves, the a and c lattice constants are both reduced by 0.4%. Choosing a smaller cutoff radius for the pseudopotential and given a converged plane-wave basis, the two lattice constants get smaller by less than 0.3%. The partial core correction[15] turns out to be important for Be. Without it the lattice constants are smaller by 1%.

A comparison of our best converged lattice parameters with the experimental values for hcp-Be shows the following. Our value for the a lattice constant, 4.21 bohr, is 2.5% smaller than the experimental value of $a = 4.32$ bohr.[43] This difference is large but still reasonable for a well-converged LDA calculation using the Ceperley/Alder potential[12] for XC.[44] The calculated c/a ratio of 1.573 is 0.4% larger than the experimental value[43] and 3.7% smaller than the ideal c/a ratio corresponding to close packing of spheres. The Poisson ratio we determine to be $\nu_P = 0.02 \pm 0.01$. This value is within the range of experimental values $(0.02 - 0.05)$.[45,46]

2. Relaxation of the Be(0001) surface

Be(0001) is the surface that shows the largest outward relaxation of the top layer, in percent of the interlayer spacing, of all the surfaces investigated yet. This was first established in a LEED analysis by Davis *et al.* ($\Delta d_{12} = 5.8\%$, see Table IV).[47] This observation was qualitatively confirmed by two first-principles calculations. Feibelman used the LAPW method and Wigner for XC and got $\Delta d_{12} = 3.9\%$.[19] Holzwarth and Zeng used a plane-wave pseudopotential (PWPP) method.[48] Within LDA they got $\Delta d_{12} = 2.1\%$, and using the generalized gradient approximation (GGA), they calculated $\Delta d_{12} = 2.5\%$. Our calculations also yield an expansion of Be(0001) ($\Delta d_{12} = 2.7\%$).

The quantitative agreement of the different results is rather poor. We first discuss the possible reasons for this disagreement which is larger than usual for modern LEED analysis and LDA calculations. Then we address the physical origin of the observed large outward relaxation.

The cause for the difference between the LAPW results of Ref. 19 and the two other calculations is for the most part the different **k** sampling. Both calculations agree reasonably well if the same set of 14 **k** points in the irreducible 1/12 of the hexagonal SBZ is used (see Table IV). The top layer relaxes outward by ca. 4% for this sampling. Using a better converged set of **k** points reduces this value to ca. 2.5%. The better **k**-point sampling can best be achieved with the orthorhombic supercell. For this cell, which contains two atoms per surface cell, already 18 **k** points in the irreducible 1/4 of the SBZ give reliable values of the relaxation as can be seen in comparison with the 72 **k**-point calculation of the same cell.[49]

The relaxation of Be(0001) is not only very sensitive to **k**-space sampling, but also to a variation of the slab thickness (see Table IV). If the goal is to get a precision of better than 0.5%, the slabs have to be as thick as 13 layers.[50] The size of the basis set is less crucial in our calculations. A change of the plane-wave cutoff from 20 Ry to 30 Ry changes the values for d_{ij} by less than 0.1.

The energy gain associated with the relaxation of Be(0001) is small, as for other close-packed surfaces.[30,51] We get a value of 6 meV per surface atom. The surface is softer than the bulk. We calculate that the force constant for vertical displacement of the top layer on Be(0001) relative to the second layer is 20% smaller than for the displacement of the third layer relative to the fourth which should be close to the bulk value.

It is unclear why experiment and theory disagree as

TABLE IV. Relaxation of outer layers of Be(0001), according to LEED analysis and to first-principles calculations. The results of the calculations are given for two different surface unit cells—hexagonal with one atom per surface cell and orthorhombic with two atoms—different **k**-space meshes, and different number of atomic layers in the slab. Always both sides of the slab were relaxed. The last row gives our best estimate for the converged LDA result.

Experiment				Δd_{12} (%)	Δd_{23} (%)	Δd_{34}(%)	
LEED (Ref. 47)				5.8	-0.2	0.2	
Theory	cell	**k** points	layers	Δd_{12} (%)	Δd_{23} (%)	Δd_{34}(%)	Δd_{45} (%)
LAPW (Ref. 19)	hex.	14	7	4.4	2.2		
			9	3.9	2.2		
PWPP, LDA (Ref. 48)	hex.	55	9	2.1			
PWPP, GGA (Ref. 48)				2.5			
This work	hex.	14	7	4.0	2.0		
			9	3.7	1.5	-0.5	
	ortho.	18	9	2.3	0.9	0.2	
			11	2.9	1.7	0.9	
			13	2.6	1.2	0.6	0.2
		72	9	2.5	0.8	0.3	
			11	2.9	1.3	0.8	
Best estimate				2.7	1.2	0.6	0.2

much as they do. The value of Davis *et al.* for the outer layer relaxation is more than 3% larger than the best converged LDA value. This could be a failure of LDA as compared to an exact treatment of the XC functional. The GGA should be a better approximation to the exact XC functional. The recent results of Holzwarth and Zeng, however, show that using the GGA instead of the LDA increases d_{12} by only 0.4%. Therefore, it is unlikely that LDA fails dramatically in the calculation of the relaxation of Be(0001).

Another explanation for disagreement between experiment and theory might be that temperature effects are not included within the theory. Temperature might induce an expansion of the outer layer separation. To investigate that, LEED spectra of Be(0001) were taken by Pohl, Hannon, Rous, and Plummer[52] at room temperature and at liquid nitrogen temperature. Those LEED spectra are almost identical. Therefore, also, the relaxation is almost identical in both cases.[37]

We can understand the agreement of room and low temperature data as a consequence of the very high Debye temperature Θ_D of Be. Experimental values for bulk-Be range from 1100 K to 1500 K.[45,47] The LEED analysis gives a value for Θ_D in the first layer that is only a few hundred K smaller than that. Vibrational anharmonicity expands the lattice noticeably only at and above the Debye temperature.

3. Relation between bonding in Be bulk and at the Be(0001) surface

a. Be bulk

Be is not a typical *sp* metal. It is a first row element and can, therefore, form the strongest bonds among the alkaline earths. Bulk hcp Be is nearly a semiconductor in its electronic and elastic properties. It has a band gap in most of the BZ. The Fermi density of states is nearly four times smaller than for a free-electron metal of the same density.[53–55] The bonds in hcp-Be are anisotropic. The bond length in the basal plane is about 3% larger than in the perpendicular (0001) direction. This leads to a c/a ratio about 4% smaller than ideal. The elastic properties are also very anisotropic.[46] The Poisson ratio, for example, is ten times smaller than for all other elements. Be is unlike nearly all metallic systems in that noncentral forces are important for an even qualitative description of lattice dynamics in the bulk.[37,42,56] This is similar to the situation in semiconductors.

b. Clean Be(0001)

The character of the Be(0001) surface is very different from the bulk. The main change is that the Fermi density of states is very close to the free-electron value in the surface layer and is still larger than in the bulk for the second and third layer.[54,55] The additional density of states originates from surface states, which extend over most of the SBZ.[19,54]

The bonding character at the surface is much more metallic than in the bulk. In a force constant model describing the vibrational properties of Be(0001) the noncentral force constants, which are essential for the bulk, can be set to zero.[37,42] This is indicative of a more isotropic screening at the surface.

The more metallic and isotropic bonding at Be(0001) also appears related to the observed expansion. Isotropic bonding means that all bonds should be equal in length. So locally at the surface the c/a ratio increases toward the ideal ratio, i.e., the surface expands. Because the surface states extend to the second and the third layer, the expansion is nonoscillatory.

It would be desirable if this explanation applied to systems other than Be(0001). It does not apply for Mg(0001) (Ref. 51) or for Al(111);[57] however, Mg and Al are good metals already in the bulk and neither surface has important surface states like Be(0001).[37]

Another consequence of the surface states at Be(0001)

TABLE V. Adsorption energy, geometry, and work function of 1 ML of H adsorbed on flat Be(0001) at three high symmetry sites. We compare our results with two previous LDA calculations (Refs. 5 and 6). We report our results for different **k**-space sampling and slab thickness. E_{ad} is the H adsorption energy relative to 1 Ry for the free H atom, d_{H-Be} is the distance between the H adlayer and the Be surface layer, Δd_{12} and Δd_{23} represent the relative outer layer expansion [compare Table IV for clean Be(0001)], and Φ is the work function [for clean Be(0001) we get $\Phi = 5.5$ eV]. Note that in Ref. 6 the Wigner form for XC (Ref. 44) and a reduced basis set are used so that only adsorption energy differences should be compared.

	Cell	**k** points	Layers	Site	E_{ad} (eV)	d_{H-Be} (bohr)	Δd_{12} (%)	Δd_{23} (%)	Φ (eV)
PWPP (Ref. 5)	hex.	12	4	fcc	1.73	1.76			
				bridge	1.82	1.85			
				hcp	1.64	1.77			
LAPW (Ref. 6)	hex.	14	7	fcc	1.23	1.75	1.4		3.9
				bridge	1.38	1.87	-0.3		3.2
				hcp	1.16	1.82	0.4		3.5
This work	hex.	14	7	fcc	1.60	1.68	2.4	-0.1	3.8
				hcp	1.51	1.74	1.3	-0.2	3.4
			9	fcc	1.59	1.69	2.7	0.1	3.8
	rect.	18	9	fcc	1.61	1.74	3.0	0.4	3.6
				bridge	1.70	1.84	2.6	0.3	3.2
				hcp (Ref. 25)	1.56	1.78	2.3	0.6	3.1

is the appearance of four distinct surface core-level shifts (SCLS).[55,58] The shift is 0.94 eV according to our calculations, more than for any other metal. The SCLS's at Be(0001) are to 75% caused by an upward shift of the potential at the surface and to 25% by the better screening of the core hole at the surface. Prominent surface states and large SCLS's are typical for semiconductor surfaces.[59]

APPENDIX B: DOES H REMOVE THE RELAXATION OF Be(0001)?

According to Ref. 6 the adsorption of a monolayer of H atoms should remove the relaxation of the Be(0001) surface. This is an effect that is often found upon adsorption of H both on semiconductor and metal surfaces.[18,29] Tables I and V show that the relaxation is not or only partially removed. The main reason is that the H adlayer does not allow the Be surface to recover its covalentlike bonding. The Fermi density of states in the surface layer after adsorption of 1 ML of H is still more than twice as high as in bulk-Be. The more metallic and isotropic bonding because of the higher Fermi density of states in the surface is the driving force for the outward relaxation. We note that as for the clean surface, careful **k**-space sampling is essential to get converged results for the relaxation of the H covered surface (compare Table V).

[1] K. B. Ray, J. B. Hannon, and E. W. Plummer, Chem. Phys. Lett. **171**, 469 (1990).
[2] K. B. Ray, X. Pan, and E. W. Plummer, Surf. Sci. **285**, 66 (1990).
[3] V. Lossev and J. Küppers, Surf. Sci. **284**, 175 (1993).
[4] K. Pohl, J. B. Hannon, and E. W. Plummer (unpublished).
[5] R. Yu and P. K. Lam, Phys. Rev. B **39**, 5035 (1989).
[6] P. J. Feibelman, Phys. Rev. B **48**, 11 270 (1993).
[7] P. J. Feibelman, Phys. Rev. Lett. **69**, 1568 (1992).
[8] A. Schmalz, S. Aminpirooz, L. Becker, J. Haase, J. Neugebauer, M. Scheffler, D. R. Batchelor, D. L. Adams, and E. Bøgh, Phys. Rev. Lett. **67**, 2163 (1991).
[9] J. Neugebauer and M. Scheffler, Phys. Rev. B **46**, 16 067 (1992); Phys. Rev. Lett. **71**, 577 (1993).
[10] S. Oppo, V. Fiorentini, and M. Scheffler, Phys. Rev. Lett. **71**, 2437 (1993).
[11] J. A. Ruffner, J. M. Slaughter, and C. M. Falco, Appl. Phys. Lett. **60**, 2995 (1992).
[12] D. M. Ceperley and B. J. Alder, Phys. Rev. Lett. **45**, 566 (1980), as parametrized by J. P. Perdew and A. Zunger, Phys. Rev. B **23**, 5048 (1981).
[13] N. Troullier and J. L. Martins, Phys. Rev. B **43**, 1993 (1991).
[14] L. Kleinman and D. M. Bylander, Phys. Rev. Lett. **48**, 1425 (1982).
[15] S. G. Louie, S. Froyen, and M. L. Cohen, Phys. Rev. B **26**, 1738 (1982).
[16] G. B. Bachelet, D. R. Hamann, and M. Schlüter, Phys. Rev. B **26**, 4199 (1982).
[17] X. Gonze, R. Stumpf, and M. Scheffler, Phys. Rev. B **44**, 8503 (1991).
[18] R. Stumpf and P. M. Marcus, Phys. Rev. B **47**, 16 016 (1993).
[19] P. J. Feibelman, Phys. Rev. B **46**, 2532 (1992).
[20] H. J. Monkhorst and J. D. Pack, Phys. Rev. B **13**, 5188 (1976).
[21] M. Methfessel and A. T. Paxton, Phys. Rev. B **40**, 3616 (1989). The main reason for using the Methfessel/Paxton method instead of the more common Fermi distribution for the electronic occupation numbers is that this way the Hellmann-Feynman forces on the atoms do not need to be corrected (Refs. 9 and 60). Details will be given elsewhere.

[22] R. Car and M. Parrinello, Phys. Rev. Lett. **55**, 2471 (1985).
[23] A. Williams and J. Soler, Bull. Am. Phys. Soc. **32**, 562 (1987).
[24] R. Stumpf and M. Scheffler, Compt. Phys. Commun. **79**, 447(1994).
[25] At the hcp site is an energy maximum. The determination of its energy while relaxing the substrate is ambiguous. If we fix the x and y coordinate of the H adsorbate to be at the hcp site and then relax the substrate atoms, the upper substrate layers move in the x-y plane out of registry.
[26] S. Wilke, D. Hennig, and R. Löber, Phys. Rev. B **50**, 2548 (1994).
[27] We use the experimental energies for the free H atom and the H_2 molecules in order to minimize the known overbinding of LDA.
[28] E. W. Plummer and P. A. Dowben, Prog. Surf. Sci. **42**, 201 (1993).
[29] K. Christmann, Surf. Sci. Rep. **9**, 1 (1988).
[30] R. Stumpf and M. Scheffler, Phys. Rev. Lett. **72**, 254 (1994); (unpublished).
[31] Using 0.14 eV as the energy barrier, $10^{-4}\,\mathrm{cm}^2/\mathrm{s}$ as the diffusion prefactor, one can estimate that the mean time between jumps is 10^{-10} s at $T = 300$ K.
[32] R. Stumpf (unpublished).
[33] J. K. Nørskov, Prog. Phys. **53**, 1253 (1990).
[34] One monolayer of H adatoms is equivalent to one H adatom per surface atom of the unreconstructed Be(0001) surface.
[35] A quasi-isolated surface vacancy on Be(0001) has a formation energy of 1.6 eV, as calculated for one vacancy per $2\sqrt{3} \times 3$ surface unit cell.
[36] C. Kittel, *Introduction into Solid State Physics*, 6th ed. (Wiley, New York, 1986).
[37] R. Stumpf, J. B. Hannon, P. J. Feibelman, and E. W. Plummer, in *Electronic Surface and Interface States on Metallic Systems*, edited by M. Donath and E. Bertel (World Scientific, Singapore, 1995).
[38] H. Polatoglou, M. Methfessel, and M. Scheffler, Phys. Rev. B **48**, 1877 (1993).
[39] We estimate the formation energy of the missing row structure on Al(111) as the sum of the two-step formation energies on Al(111) (Ref. 30). The estimate should be rather accurate because the step formation energy is relatively independent of the step-step separation on Al(111) (Ref. 30).
[40] We do not have an explanation for this very large difference in vacancy formation energy between Be(0001) and Al(111) surfaces. It is especially unclear why the energy to form the honeycomb vacancy array is so small on Al(111). This question will be the subject of a forthcoming paper.
[41] R. Stumpf and P. J. Feibelman (unpublished).
[42] E. W. Plummer and J. B. Hannon, Prog. Surf. Sci. **46**, 149 (1994).
[43] V. M. Amonenko, V. Y. Ivanov, G. F. Tikinshkiy, and V. A. Finkel, Phys. Metall. Metalloved. **14**, 47 (1962).
[44] The Wigner interpolation formula for XC [E. Wigner, Phys. Rev. **46**, 1002 (1934)] as done in Refs. 19 and 6 generally gives longer bonds and a smaller energy per bond. E.g., we find lattice constants which are larger by 1.4 % with Wigner as compared to Ceperley and Alder (Ref. 12).
[45] J. F. Smith and G. L. Arbogast, J. Appl. Phys. **31**, 99 (1960).
[46] D. J. Silversmith and B. L. Averbach, Phys. Rev. B **1**, 567 (1970).
[47] H. Davis, J. Hannon, K. Ray, and E. W. Plummer, Phys. Rev. Lett. **68**, 2632 (1992).
[48] N. A. W. Holzwarth and Y. Zeng (to be published); as LDA they use Ceperley and Alder (Ref. 12), as GGA they use J. P. Perdew, J. A. Chevary, S. H. Vosko, K. A. Jackson, M. R. Pederson, D. J. Singh, and C. Fiolhais, Phys. Rev. B **46**, 6671 (1992).
[49] The key to an understanding of the sensitivity of the value of the relaxation with the **k**-space sampling is the concentration of the surface density of states around the K point of the SBZ. This is poorly sampled by the **k**-point meshes in a hexagonal cell, because it is a high symmetry point. The surface states in turn provide for the driving force of the outward relaxation. A more detailed discussion of the physics of the outward relaxation is published elsewhere (Ref. 37).
[50] Two other surface quantities of interest are not as sensitive to computational details. One is the work function, which we determine to be 5.52 eV as compared to calculated 5.54 eV in Ref. 19. The other quantity is the surface energy per surface atom. We get 0.56 eV/atom, Holzwarth and Zeng (Ref. 48) have 0.57 eV/atom in LDA and 0.56 eV/atom in GGA, Feibelman (Ref. 19), using Wigner XC, gets 0.52 eV/atom.
[51] P. T. Sprunger, K. Pohl, H. L. Davis, and E. W. Plummer, Surf. Sci. **297**, L48 (1994); A. F. Wright, P. J. Feibelman, and S. R. Atlas, *ibid.* **302**, 215 (1994).
[52] K. Pohl, J. B. Hannon, P. J. Rous, and E. W. Plummer, Bull. Am. Phys. Soc. **39**, J75 (1994).
[53] M. Y. Chou, P. K. Lam, and M. L. Cohen, Phys. Rev. B **28**, 4179 (1983).
[54] E. V. Chulkov, V. M. Silkin, and E. N. Shirykalov, Surf. Sci. **188**, 287 (1987).
[55] P. J. Feibelman and R. Stumpf, Phys. Rev. B **50**, 17480 (1994).
[56] A. P. Roy, B. A. Dasannacharya, C. L. Thaper, and P. K. Iyengar, Phys. Rev. Lett. **30**, 906 (1973).
[57] H. B. Nielsen and D. L. Adams, J. Phys. C **15**, 615 (1982); J. R. Noonan and H. L. Davis, J. Vac. Sci. Technol. A **8**, 2671 (1990).
[58] L. I. Johansson, H. I. P. Johansson, J. N. Andersen, E. Lundgren, and R. Nyholm, Phys. Rev. Lett. **71**, 2453 (1993).
[59] F. Bechstedt and R. Enderlein, *Semiconductor Surfaces and Interfaces* (Akademie Verlag, Berlin, 1988).
[60] M. J. Gillan, J. Phys. Condens. Matter **1**, 689 (1989).

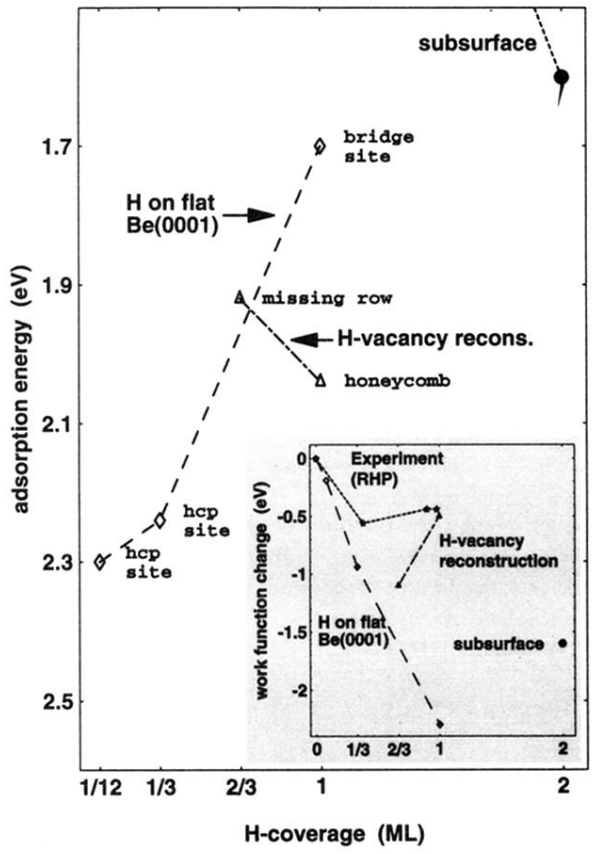

FIG. 1. H adsorption energy as a function of coverage for the three different H on Be(0001) phases discussed in the text; the inset shows the corresponding work function changes and compares it with the experimental values of RHP (Ref. 1).